Inwardly rectifying currents in hair cells and supporting cells in the goldfish sacculus

Izumi Sugihara and Taro Furukawa

Department of Physiology, Tokyo Medical and Dental University School of Medicine, 1-5-45 Yushima, Bunkyo-ku, Tokyo 113, Japan

1. Inwardly rectifying ionic currents were studied using patch-clamp recording methods in oscillatory-type and spike-type hair cells and supporting cells dissociated from the goldfish sacculus. These cells had different types of inwardly rectifying currents. The biophysical properties of these currents were investigated.

2. A unique potassium current (I_{sc}) was the sole ionic current recognized in supporting cells. I_{sc} was active throughout the membrane potential range between +30 and −170 mV, but showed weak inward rectification and no inactivation.

3. In spike-type hair cells, inwardly rectifying current (I_{K1}) was selectively permeable to K^+ (K^+:Na^+ permeability ratio, 1:0·0021). I_{K1} could underlie the high negative resting potential of these hair cells because it is partially active at this potential. The strong inward rectification of I_{K1} contributed to the low negative plateau potential seen in spike-type hair cells.

4. In oscillatory-type hair cells, hyperpolarization-activated potassium–sodium current (I_h), which had properties similar to that in photoreceptor and other neurons, was present instead of inwardly rectifying K^+ current.

5. In the cell-attached and inside-out modes with 125 mM external K^+ ($[K^+]_o$), I_{K1} channel had a unitary conductance of 27 pS and showed inactivation with increasing hyperpolarization. Putative I_h and I_{sc} single channels had unitary conductances of 7 and 61 pS, respectively, in the cell-attached mode with 125 mM K^+_o.

In the goldfish saccular macula, as in other hair cell organs, hair cells are surrounded by supporting cells (Hama, 1969). These two kinds of cells constitute the sensory epithelium. While hair cells transduce mechanical stimuli, sound in the case of the goldfish sacculus (Furukawa & Ishii, 1967), supporting cells are the less active constituent of the sensory epithelium.

Saccular hair cells have been classified, based on patch-clamp studies in isolated cells, into oscillatory and spike types (Sugihara & Furukawa, 1989). Oscillatory-type hair cells are located in the rostral and caudal sacculus and are short or ovoid in shape, while long spike-type hair cells are found only in the caudal sacculus (Sugihara & Furukawa, 1989). No comparable patch-clamp study has been carried out in supporting cells. However, using an *in situ* preparation, Furukawa (1985) obtained intra- and extracellular electrical recordings from supporting cells in the rostral region of the saccular macula of goldfish. His results on sound-evoked DC potentials suggested that these supporting cells have K^+ conductance, as do glial cells in the central nervous system (Orkand, Nicholls & Kuffler, 1966) and Müller cells in the retina (Newman, 1985, 1993). Similar, but much smaller, sound-evoked DC potentials have been obtained from supporting cells in the guinea-pig cochlea (Oesterle and Dallos, 1990).

In cell preparations dissociated from the goldfish saccular macula, supporting cells can be identified morphologically. In this report, we show for the first time that supporting cells have a unique inwardly rectifying K^+ conductance (designated I_{sc}). In comparison, hair cells have different inwardly rectifying currents: spike-type hair cells have inwardly rectifying K^+ current (I_{K1}) and oscillatory-type hair cells have another inwardly rectifying current, which is similar to the hyperpolarization-activated K^+–Na^+ current (I_h) reported in photoreceptors (Sugihara & Furukawa, 1989).

We also investigate the detailed biophysical properties, including single-channel activities, of these three different kinds of inwardly rectifying current (I_{sc}, I_{K1} and I_h) that are expressed in supporting cells and the two kinds of hair cells. We discuss here the possible functional significance of I_{sc} in supporting cells in buffering the extracellular K^+ concentration. We propose here that strict inward rectification of I_{K1} may facilitate the low negative plateau potential seen in spike-type hair cells.

METHODS

Preparation and experiments

Detailed procedures for preparing single cells from the inner ear of goldfish, *Carassius auratus*, have been described previously (Sugihara & Furukawa, 1989; Sugihara, 1994). Goldfish were anaesthetized with an intramuscular injection of ketamine hydrochloride (1 mg (g body weight)$^{-1}$). The dorsal skull and the brain were removed to excise the inner ear structures. Hair cells and supporting cells were isolated from the saccular maculae.

Patch-clamp experiments were performed using an EPC-7 amplifier (List Electronic) as described previously (Sugihara, 1994; Sugihara & Furukawa, 1995). The cut-off frequency was 5 or 1 kHz (−3 dB; 4 pole Bessel filter, about 24 dB octave^{-1}) and the sampling period of digitizing was 40 or 250 μs, for voltage- or current-clamp recording, respectively, unless otherwise indicated. Neither subtraction for leakage or capacitive currents nor averaging was applied to the whole-cell voltage-clamp records. To measure the time constant, a single-exponential curve was fitted to the rising or decay phase of the current record using the maximum likelihood method with Simplex minimization (Dempster, 1993). To measure unitary amplitude, two Gaussian curves were fitted on the amplitude histogram of single-channel records. The values are presented as means ± S.D.

Solutions

The compositions of the bath and pipette solutions were as follows (mM). Normal Ringer solution: NaCl, 120; KCl, 2; $CaCl_2$, 2; Hepes, 5; NaOH 1·5. This solution was used for the bath in cell-attached and whole-cell clamp recordings. The internal (pipette) solution for whole-cell clamp recordings was one of the following three solutions. KCl internal solution: KCl, 105; Hepes, 5; EGTA, 5; KOH, 20. Potassium citrate internal solution: potassium citrate, 53; Hepes, 5; EGTA, 5; KOH, 20. Potassium acetate internal solution: potassium acetate, 105; Hepes, 5; EGTA, 5; KOH, 20. Among these three internal solutions, potassium acetate and potassium citrate internal solutions were mostly used in earlier experiments. The K^+ concentration of the potassium citrate solution (179 mM) is higher than those of other solutions (125 mM) because citrate is trivalent, although the total ionic molarity is similar. For recordings in the inside-out mode, 125 mM KCl solution without EGTA (KCl, 125; Hepes, 5; KOH, 1·5) was used for both the pipette and the bath. In the cell-attached mode, this 125 mM KCl solution or one of the internal solutions for whole-cell recording was used in the pipette. For all the solutions, the pH was adjusted to 7·2 with a small amount of HCl, NaOH or KOH. The liquid junction potentials of KCl, potassium citrate, potassium acetate internal solutions and KCl inside-out solution against normal Ringer solution were −5, −15, −10 and −4 mV, respectively. The K^+ concentration in the bath ($[K^+]_o$) was changed by isomolar replacement with Na^+ in reversal potential experiments.

RESULTS

Morphology of dissociated supporting cells

Supporting cells were identified morphologically by a tall bipolar shape with a narrow centre and swelled bulb-like ends, one of which (basal side) was slightly larger than the other (Fig. 1*A* and *B*). These cells were solitary or sometimes attached to a hair cell at the border between the apical and basolateral surface of both cells (Fig. 1*A*). This is where the tight junction is located between neighbouring hair cells and supporting cells (Hama, 1969). The supporting cells were 48·2 ± 9·4 μm (mean ± S.D., $n = 6$) long and 2·0 ± 0·4 and 7·7 ± 1·1 μm wide at the centre and thicker end, respectively ($n = 6$). They were much taller than hair cells (Fig. 1*A*). The tall shape of dissociated supporting cells agrees with the findings by electron microscopy (Hama, 1969); supporting cells reach the basal lamina while hair cells do not.

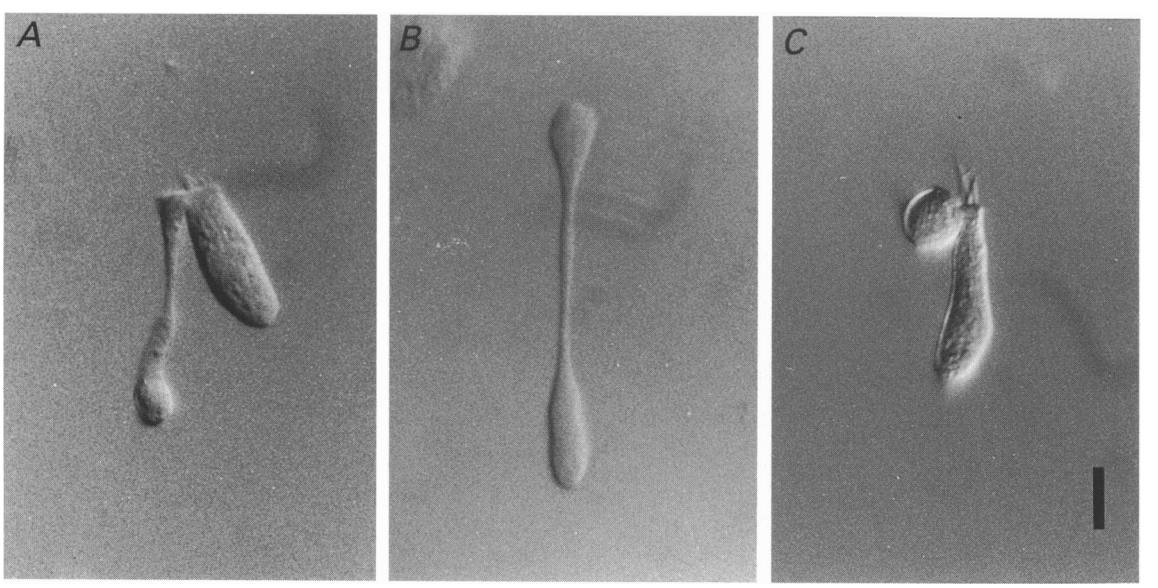

Figure 1. Photomicrographs of supporting cells dissociated from the goldfish saccular macula

A, a tall supporting cell (left) attached to a hair cell (right). *B*, a solitary tall supporting cell. *C*, a round supporting cell attached to a hair cell. Scale bar represents 10 μm. Nomarski differential interference optics were used.

Other type of cells that were attached to hair cells were round with a diameter of 9·4 ± 0·8 μm ($n = 14$) (Fig. 1*C*). The attachment was again always at the border between the apical and basolateral surface of the hair cells (Fig. 1*C*), indicating that the connection between the two cells was reminiscent of the original structure. Therefore, these round cells were very likely to be supporting cells that had been deformed by dissociation treatment (designated 'round' supporting cells in contrast with the typical 'tall' supporting cells). Recordings were made from tall supporting cells that were either solitary or attached to hair cells, and round supporting cells attached to hair cells dissociated from the caudal sacculus, since the rostral sacculus gave far fewer isolated cells.

Ionic current of supporting cells

Tall and round supporting cells had a zero-current potential of −78·2 ± 5·7 mV ($n = 4$) and −74·5 ± 5·0 mV ($n = 6$), respectively, measured with potassium acetate or potassium citrate in the pipette. These values were similar to the resting potential of supporting cells recorded in *in vivo* experiments (−70·6 mV, Furukawa, 1985). Input resistance and input capacitance were 671 ± 455 MΩ and 5·2 ± 2·3 pF ($n = 4$), and 694 ± 407 MΩ and 2·9 ± 0·24 pF ($n = 6$) for tall and round cells, respectively.

The ionic current of supporting cells was examined by applying depolarizing or hyperpolarizing command voltages in voltage-clamp mode. Records obtained in a tall and a round supporting cell are shown in Fig. 2*A*. The current

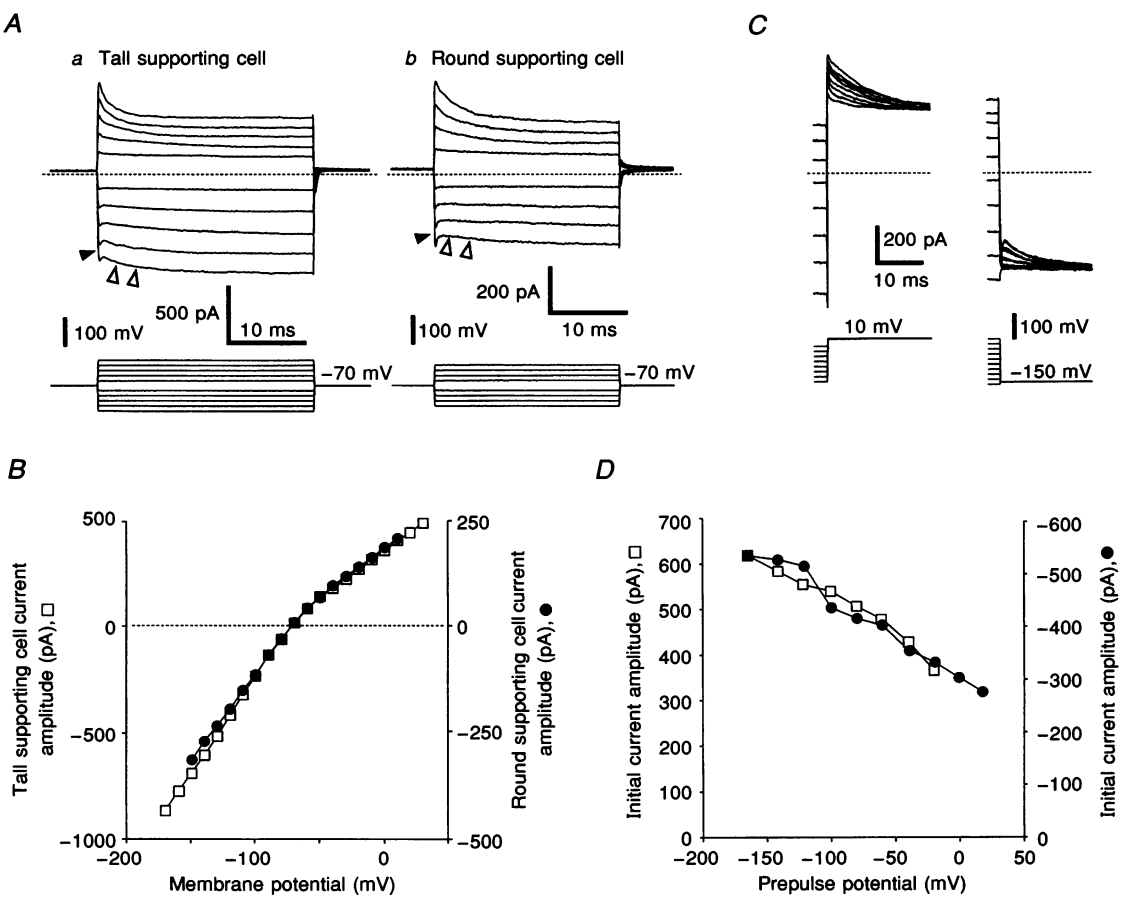

Figure 2. Inwardly rectifying current (I_{sc}) of tall and round supporting cells

A, current records obtained by applying voltage pulses (duration, 25 ms) of different amplitudes ranging from ±20 to either ±80 mV or ±100 mV (holding potential, −70 mV) in tall (*a*) and round (*b*) supporting cells. Filled and open arrowheads indicate instantaneous and time-dependent activation of the current, respectively. *B*, current–voltage relationship for the traces depicted in *A* at the end of the pulse for tall (□) and round supporting cells (●). Different ordinate scales were used for comparison. *C*, records of current relaxation (tail current) obtained by applying prepulses (duration, 30 ms) of different amplitudes between −20 (+20, right) and −160 mV followed by command pulses of +10 mV (left) and −150 mV (right) in the same tall supporting cell as depicted in *A a*. *D*, initial current amplitude at the onset of the command pulse plotted against the prepulse potential using the data depicted in *C* (+10 mV, □; −150 mV, ●). Different ordinate scales were used for comparison. The initial amplitude was measured by fitting a single-exponential curve on the relaxation time course of the current. Potassium acetate internal solution was used. Dashed lines indicate the zero-current level.

recorded from the two types of supporting cells were nearly identical (Fig. 2*A a* and *b*). Depolarizing voltage jumps evoked instantaneous outward current which gradually decayed to a certain extent. This instantaneous activation of the outward current due to a sudden change in the driving force suggests that the underlying conductance was already active at the holding voltage. The decay of the outward current during the pulse could be regarded as relaxation to a new steady state. The decay ceased in about 10–20 ms and a steady-state outward current remained. The time course of the decay of the outward current was accelerated with augmentation of depolarization (the time constant was 11·2 and 2·4 ms for −50 and +30 mV, respectively, in the tall cell in Fig. 2*A a*).

Hyperpolarizing voltage steps elicited the instantaneous appearance of inward current (filled arrowheads in Fig. 2*A a* and *b*) and a further time-dependent increase (open arrowheads in Fig. 2*A a* and *b*) in inward current. While the former was produced by the sudden increase in the driving force, the latter represented relaxation towards a new steady state, in which the conductance of this current is greater than that in the holding potential. The time course of the increase in the inward current was accelerated with increasing hyperpolarization (the time constant was 26·6 and 4·3 ms for −90 and −170 mV, respectively, in the tall cell). A small inward surge at the onset of the voltage steps was presumably uncancelled capacitive current. In contrast to I_{K1}, this current in supporting cells did not show time-dependent decay (inactivation) at high negative potentials.

The current–voltage (*I–V*) relationships measured from the current amplitude in the steady state at the end of the command pulse were nearly identical for the tall and round supporting cells (Fig. 2*B*). The curves both had a simple convex shape, i.e. the slope of the curve decreased with depolarization (Fig. 2*B*), implying the prominence of inward rectification. It is very likely that the outward current and inward current were carried by the same conductance, for several reasons. First, the overall shape of the *I–V* relationship was uniformly convex with no inflection point. Second, the ratio of the intensities of outward and inward current (cf. Fig. 2*B*) was similar across different cells ($n = 10$). This current was designated I_{sc}, '(inwardly rectifying) current of supporting cells.' The *I–V* relationship obtained by applying slow ramp-shaped wave voltage changes around the zero-current potential (not shown) had a convex shape without hysteresis, similar to that obtained with voltage steps, indicating that there was no slow inactivation process in I_{sc}.

Voltage dependence of I_{sc}

Voltage dependence of I_{sc} was measured by a prepulse protocol. A 30 ms prepulse of various amplitudes was applied prior to the depolarizing command pulse to 10 mV (Fig. 2*C*, left panel). The initial amplitude of the outward current measured at the onset of the command pulse should represent the extent of I_{sc} activation at the preceding prepulse potential. Figure 2*C* (left panel) shows that greater hyperpolarization in the prepulse potential produced a greater instantaneous outward current. Similar measurements were made with a command pulse of −150 mV (Fig. 2*C*, right panel), in which greater depolarization of the prepulse produced a smaller instantaneous inward current.

The plots of instantaneous current amplitude against the prepulse potential (voltage-activation curves) for command voltages of +10 and −150 mV could be superimposed on

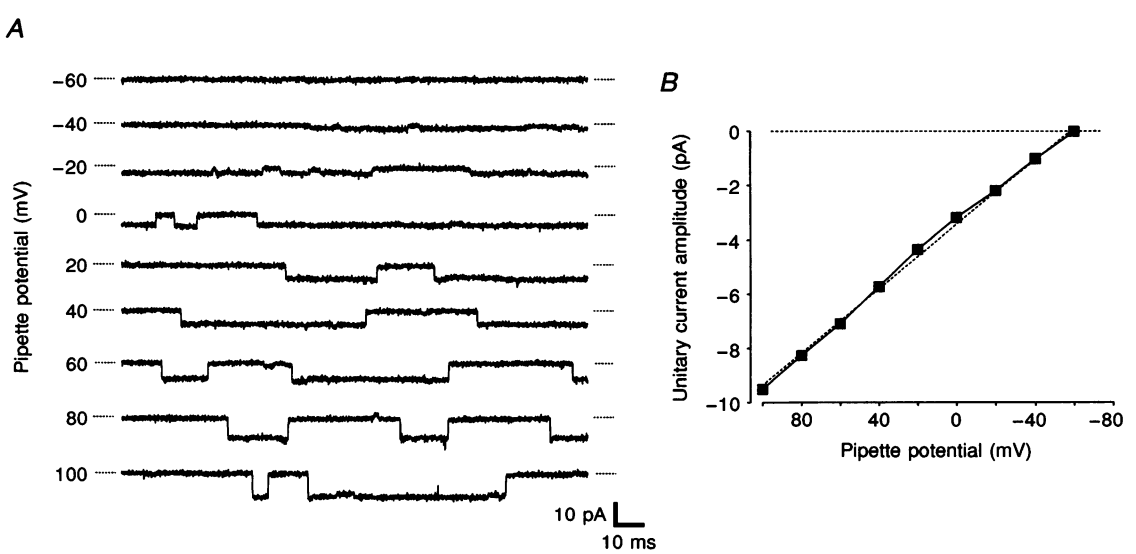

Figure 3. Single-channel current of I_{sc} recorded in the cell-attached mode

A, current traces recorded from a cell-attached patch in a round supporting cell. The pipette potential for each trace is presented. Dashed lines indicate the shut level. *B*, single-channel amplitude of the channel shown in *A* plotted against the pipette potential. The fitted straight line (slope = 60 pS) was obtained by the least-squares method. The pipette solution was potassium acetate.

each other by using a different ordinate scale (Fig. 2*D*). Furthermore, the slopes of the two plots were roughly constant over all measured prepulse voltage ranges. These results support the previous interpretation that the outward current and inward current flow through the same conductance, I_{sc}. The plots clearly indicated that the activity of I_{sc} waned gradually as the membrane potential shifted in the positive direction, which was the basis for the weak inward rectification of I_{sc}. This voltage dependence of I_{sc} may be due to voltage-dependent activation and deactivation or to depolarization-dependent blockade.

Since the internal solution we used did not contain Mg^{2+} or polyamines, which are responsible for rectification in many inwardly rectifying K^+ channels (Matsuda, Saigusa & Irisawa, 1987; Lopatin, Makhina & Nichols, 1994), the rectification of I_{sc} in the physiological condition could be more pronounced. However, it was obvious that the rectification of I_{sc} was much weaker than that of I_{K1} (see later sections) in the present study.

K^+ selectivity and pharmacology of I_{sc}

The effect of changing $[K^+]_o$ on the zero-current potential was measured in one round supporting cell. Potassium acetate solution was used in the pipette. With $[K^+]_o$ of 2, 5 and 10 mM, the zero-current potential was −78, −68 and −55 mV. These points were fitted well by the Goldman–Hodgkin–Katz equation assuming predominant K^+ as well as slight Na^+ permeability (K^+ : Na^+ permeability ratio, 1 : 0·027). Neither 4-aminopyridine (4-AP, 3 mM, $n = 2$ cells) nor tetraethylammonium (TEA, 30 mM, $n = 1$ cell) blocked the current when added to the bath.

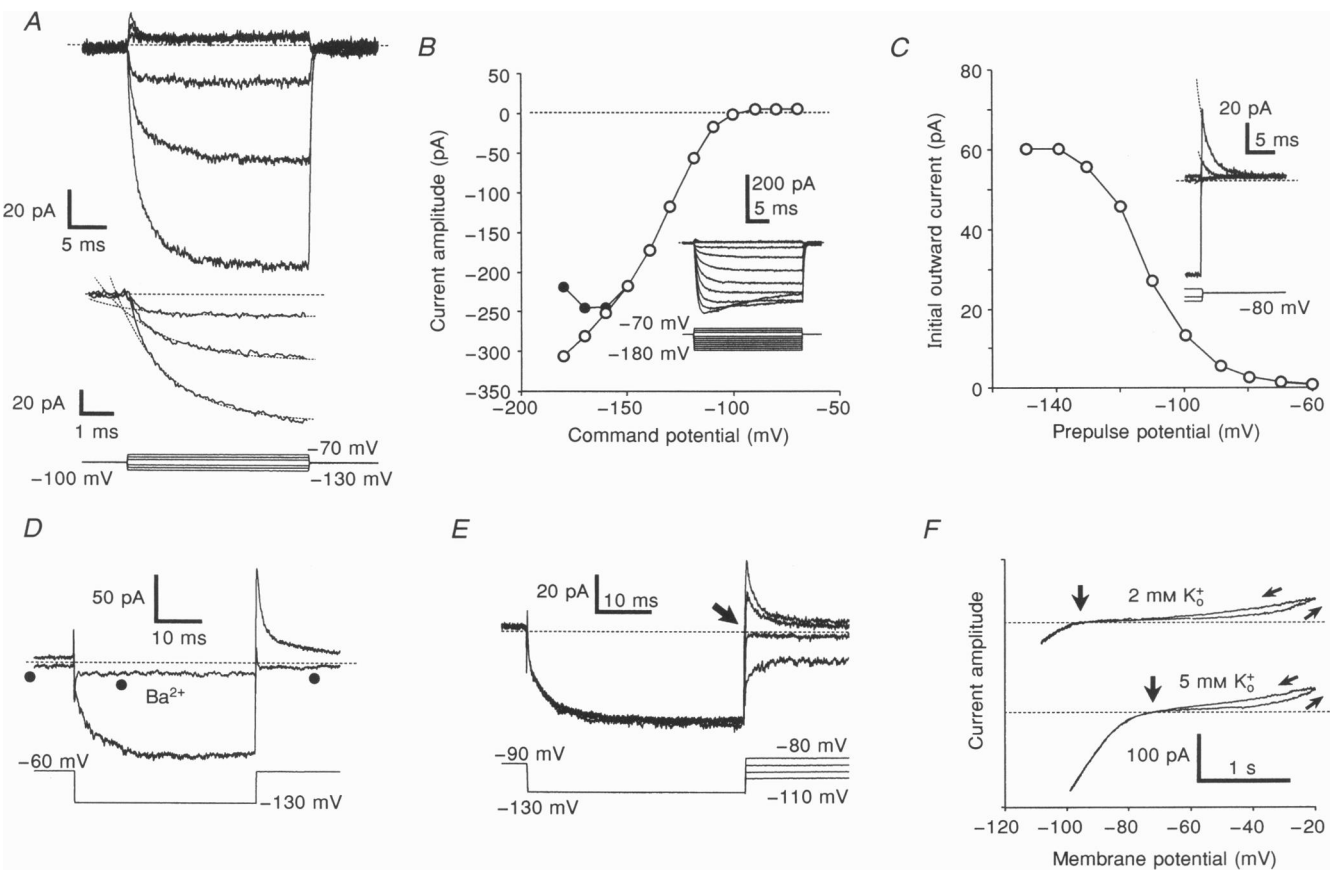

Figure 4. Inwardly rectifying K^+ current (I_{K1}) in spike-type hair cells

A, I_{K1} recorded in a slender spike-type hair cell from the caudal saccule. In the bottom inset, the initial portions of the inward current activated in response to potential steps are shown. Single-exponential curves (time constant, 1·5, 1·8 and 1·6 ms for −10, −20 and −30 mV steps, respectively) were fitted to the region from 0·5 to 3·5 ms after the onset of the step. *B*, *I–V* relationship of I_{K1} (peak value, ○; value at the end of 25 ms pulse, ●) obtained from the same cell as shown in *A*. *C*, initial amplitude of decaying outward current measured by applying prepulses of different amplitudes followed by a command pulse of −80 mV. *D*, current traces recorded before and after adding Ba^{2+} (1·6 mM) to the bath of normal Ringer solution. *E*, reversal of the decaying current of I_{K1}. *F*, *I–V* relationship in different $[K^+]_o$ measured by applying slow ramp waves from a holding potential of −60 mV before and after increasing $[K^+]_o$ from 2 to 5 mM. Records were filtered at 100 Hz and sampled at 500 Hz. The pipette solution was KCl (*A–C*) and potassium acetate (*D*, *E* and *F*). Tetrodotoxin (0·3 μM) was added to the bath to prevent activation of Na^+ current. The zero-current levels are indicated by dashed lines.

I_{sc} channel recorded in the cell-attached mode

Single-channel current was observed in five of the eighteen cell-attached patches on the basolateral side of round and tall supporting cells with potassium acetate or potassium citrate internal solutions in the pipette. No obvious single-channel events were seen in the other thirteen patches. Single-channel events were characterized by an inward current with relatively slow gating kinetics (Fig. 3*A*). The steady-state activity of this channel was observed even at very negative potentials (bottom trace in Fig. 3*A*), indicating the absence of inactivation. The *I–V* relationship of the unitary current amplitude was nearly linear (Fig. 3*B*). Fitting to a straight line produced a reversal pipette potential of −58 mV. This value was not very different from the resting potential of supporting cells (about −70 mV) measured *in vivo* (Furukawa, 1985). Since the pipette solution had a high K^+ concentration (125 mM), this reversal potential was roughly consistent with that for a K^+ channel. The single-channel conductance measured from the slope of the fitting line was 60 pS. Similar single-channel events were observed in other cell-attached patches (unitary conductance, 61 ± 5 pS, $n = 5$; 4 round and 1 tall supporting cell).

These channels were likely to be I_{sc} channels because of the similarity of biophysical properties, such as the passage of K^+ current and the absence of inactivation. In addition I_{sc} was the sole ionic current recognized in whole-cell clamp mode in cells in which these channels were recorded in the cell-attached mode.

Inwardly rectifying K current in spike-type hair cells

Spike-type hair cells in the goldfish sacculus all had a large inwardly rectifying K^+ current (Sugihara & Furukawa, 1989). We refer to this current as I_{K1}, which is consistent with the terminology used for similar currents in cardiac cells and frog hair cells (Holt & Eatock, 1995). In the present study, the activity of this current around and above the resting potential was examined in detail. Figure 4*A* shows current records from a spike-type hair cell. The holding potential was −100 mV, which was approximately equal to the zero-current potential. Hyperpolarizing potential steps activated the inward current. Single-exponential curves showed a good fit to the initial portion of the activation time course, except for the very beginning (Fig. 4*A*, inset). This initial poorly fitted portion was considered to represent an instantaneous change in the current.

Small depolarizations to −70 and −80 mV elicited decaying outward current (Fig. 4*A*). The instantaneous activation of this decaying outward current, if considered together with the possible instantaneous component of the hyperpolarization-activated inward current, suggests that I_{K1} conductance was active to a certain degree at the holding

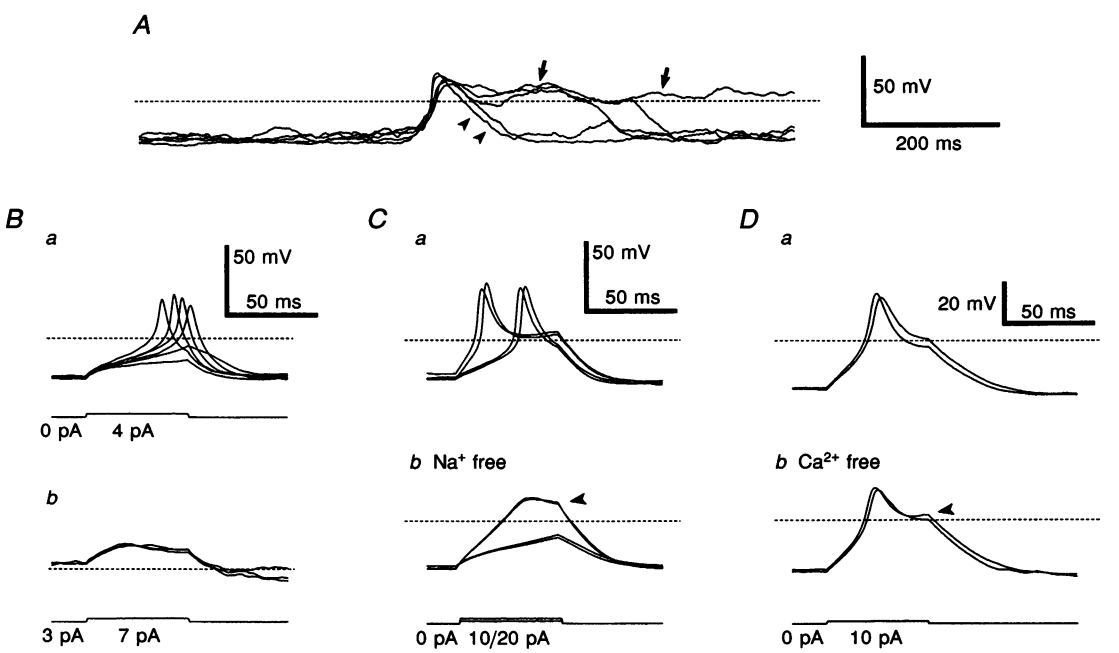

Figure 5. Low negative plateau potential in spike-type hair cells

A, spontaneous action potentials which were sometimes followed by a low negative plateau potential. Traces recorded in the current-clamp mode were superimposed arbitrarily. *B*, all-or-none spike responses evoked by the injection of 4 pA (*a*) were inhibited after switching the membrane potential to the low negative plateau level by continuous injection of 3 pA (*b*). *C*, spike responses (*a*) were largely inhibited after replacing Na^+ in the bath with choline (*b*). However, the plateau potential still remained (arrowhead in *b*). *D*, spike responses before (*a*) and after (*b*) replacing Ca^{2+} in the bath with Mg^{2+}. Arrowhead in *b* indicates the remaining plateau potential. Potassium citrate internal solution was used in the pipette (*A–D*). Dashed line, −70 mV.

potential. The decaying outward current was followed by steady small outward current (Fig. 4*A*, top traces). The amplitude of the latter was 10·6 ± 8·2 pA ($n = 20$) at −70 mV. Since the amplitude of the small steady outward current did not increase with increasing depolarization between −90 and −70 mV (Fig. 4*A*), this outward current could not be depolarization-activated outward K^+ currents. However, it could be interpreted as outward current through I_{K1} conductance. The blockade of both the small steady outward current and the inward current by the application of 1·6 mM Ba^{2+}, a blocker of I_{K1} (Carmeliet, 1982; Sakmann & Trube, 1984; Stelling & Jacob, 1992; Holt & Eatock, 1995), in the bath also indicated that the small outward current was I_{K1} (Fig. 4*D*). The decaying outward current which flowed after the offset of the hyperpolarizing potential step was also blocked by Ba^{2+} (Fig. 4*D*), indicating that this current is also I_{K1}. The decaying outward current of I_{K1} has been reported in heart muscle cells (Matsuda *et al.* 1987) and recorded in frog hair cells (Holt & Eatock, 1995). We assumed that the initial amplitude of the decaying outward current reflects the degree of I_{K1} activation at the preceding potential, as if it were a tail current. However, the term 'tail current' may not be appropriate if the decay of the current was due to blockade by Mg^{2+} and polyamines inside the cell (Matsuda *et al.* 1987; Lopatin *et al.* 1994). Measurement of the initial amplitude of the decaying outward current by changing the prepulse potential showed that I_{K1} is partially active at −90 or −100 mV (resting potential ranges of spike-type hair cells, see Sugihara & Furukawa, 1989) but is scarcely active at potentials near or above −70 mV (Fig. 4*C*). This is consistent with the very small outward current at potentials above the zero-current level in the *I–V* relationship (Fig. 4*B*), and indicates strict inward rectification of I_{K1}.

Since the internal solution we used lacked Mg^{2+} and polyamines, our observation of strict inward rectification appears to conflict with the idea that these substances produce rectification. However, we do not know if the internal solute of the cell was completely dialysed within the recording period (usually less than 10 min). Strict inward rectification of I_{K1} has also been observed with a Mg^{2+}-free internal solution in chick vestibular hair cells (Ohmori, 1984). In cases in which 1 mM $MgCl_2$ was added to the potassium citrate internal solution, the time course and *I–V* relationship of I_{K1} were similar to those recorded with Mg^{2+}-free solutions. The zero-current potential was −92·2 ± 3·1 mV ($n = 3$). The decaying outward (tail) current could not be studied in these cases because the cells were not intact for a long enough time.

K^+ selectivity of I_{K1}

The reversal potential of this current was about −100 mV when measured by changing the repolarization potential between −80 and −110 mV (Fig. 4*E*). This value was close to, but less negative than, the equilibrium potential of K^+ (−103 mV for potassium acetate in this case). If we assume permeation of Na^+ in addition to that of K^+, since Na^+ is the most abundant ion in the bath, the K^+: Na^+ permeability ratio calculated using the Goldman–Hodgkin–Katz equation is 1: 0·0021.

The effects of changing $[K^+]_o$ (from 2 to 5 mM) are shown in the *I–V* curves obtained by applying slow ramp waves (Fig. 4*F*). The general shapes of these curves indicate strict inward rectification at either $[K^+]_o$ in membrane potentials around and more positive than the zero-current level. The zero-current potentials (−96 and −72 mV for 2 and 5 mM, respectively) were slightly more positive than the K^+ equilibrium potentials (−103·0 and −80·2 mV). The zero-current potential and the conductance for the inward current were strongly dependent on $[K^+]_o$. This result agrees with the previous conclusion that I_{K1}, which has strong K^+ selectivity, constitutes substantial conductance at potentials around the zero-current level. Thus, I_{K1} underlies the high negative resting potential of spike-type hair cells.

Low negative plateau potential and inward rectification in spike-type hair cells

Some spike-type hair cells occasionally generated spontaneous spikes (Sugihara & Furukawa, 1989). This phenomenon was observed with either potassium citrate or KCl internal solutions in a small number of spike-type cells ($n = 9$ out of 69). The repolarization phase of the spontaneous spikes was slow (arrowheads in Fig. 5*A*), indicating a lack of large K^+ conductance during this period. Furthermore, spontaneous spikes were sometimes followed by low negative plateau potential (arrows in Fig. 5*A*). When a spike was elicited by an injection of positive current, the plateau potential always followed the spike as long as the current injection continued (Sugihara & Furukawa, 1989). The level of the plateau potential was about −70 to −60 mV when no current was injected (Fig. 5*A*) but could be more positive depending on the amount of current injected (Fig. 2*B* of Sugihara & Furukawa, 1989), whereas the high negative resting potential of spike-type hair cells is generally between −90 and −100 mV (Sugihara & Furukawa, 1989). Small continuous inward current could switch the membrane potential from the very negative resting level to the low negative plateau level (Fig. 5*B*). The spike could not be triggered from the plateau potential because of the inactivation of Na^+ current (Fig. 5*B*).

When Na^+ was removed from the bath, the spike response was significantly reduced while the plateau potential was still generated (Fig. 5*C*, arrowhead). Removal of Ca^{2+} from the bath caused a smaller reduction of the spike response but also did not change the plateau potential (Fig. 5*D*, arrowhead). These effects of the removal of Na^+ and Ca^{2+} were reversible, and were observed in all examined cases ($n = 4$ and 5 for Na^+ and Ca^{2+}, respectively). These results indicated that the plateau potential was not directly related to Na^+ or Ca^{2+} currents, whereas spike generation depends on Na^+ and Ca^{2+} currents. On the other hand, generation of the plateau potential can be simply explained from the *I–V* curve. The *I–V* curve is nearly flat in the potential ranges

between −50 and −100 mV (Fig. 4*F*, top) due to strict inward rectification of I_{K1}. Therefore, if a small inward current is injected, the membrane potential should settle around the rightward inflection point in the *I–V* curve produced by the depolarization-activated outward K^+ currents. Thus, the strict inward rectification of I_{K1} is indispensable for production of the low negative plateau potential. Since the depolarization-dependent outward K^+ currents were generally small in spike-type hair cells (Sugihara & Furukawa, 1989), the outward inflection in the *I–V* curve was not very sharp (Fig. 4*F*). This can explain why the plateau level changes depending on the amount of current injected.

The plateau potential in spike-type hair cells was not very stable. Without the continuous injection of positive current, the membrane potential eventually shifted from the low negative plateau level to the high negative resting level (Fig. 5*A*). Either an N-shaped *I–V* curve with three voltage-axis intercepts or a hysteretic *I–V* curve with two voltage-axis intercepts is necessary for stable dual membrane potentials (Carmeliet, 1982). However, the *I–V* curve in spike-type hair cells did not show either an N-shape or hysteresis in potential ranges below −70 mV (Fig. 4*F*). The hysteresis seen at more positive potential ranges (Fig. 4*F*) was actually opposite to that which would stabilize the plateau potential in relation to the preceding voltage. This hysteresis, caused by the tail current of depolarization-activated outward K^+ conductance, would favour the return of the membrane potential to the very negative resting level.

I_{K1} channel activity recorded in the cell-attached and inside-out modes

In cell-attached patches on a basolateral surface of long spike-type hair cells with a patch pipette filled with one of the K^+ solutions, inwardly rectifying ionic channels were often very active ($n = 119$ out of 145). By applying a slow ramp wave of potential changes, the *I–V* relationship of this activity was measured (Fig. 6*A*). The channel activity indicated by a noisy inward current was marked when the pipette potential was between about −40 and + 30 mV. However, large hyperpolarization of the patch membrane (pipette potential > +40 mV) resulted in disappearance of the current, due to decay of the channel activity at large hyperpolarization. When depolarized, no obvious outward current of similar channel activity was seen. It was not possible to observe clear, step-like open and shut events of the channels in the steady state, even with a fast time resolution. This may have been due to the very brief duration of individual open events and the presence of multiple channels.

When large hyperpolarizing potential steps were applied, the time-dependent decay of channel activity was apparent (Fig. 6*B*). Openings of the single channel were occasionally observed (Fig. 6*C*) immediately before all the channels disappeared. The slope conductance of single-channel current measured from this activity was 27·1 ± 1·8 pS (mean ± S.D., $n = 11$, with 125 mM KCl solution in the pipette) and the extrapolated reversal potential was −60·3 ± 6·6 mV (pipette potential).

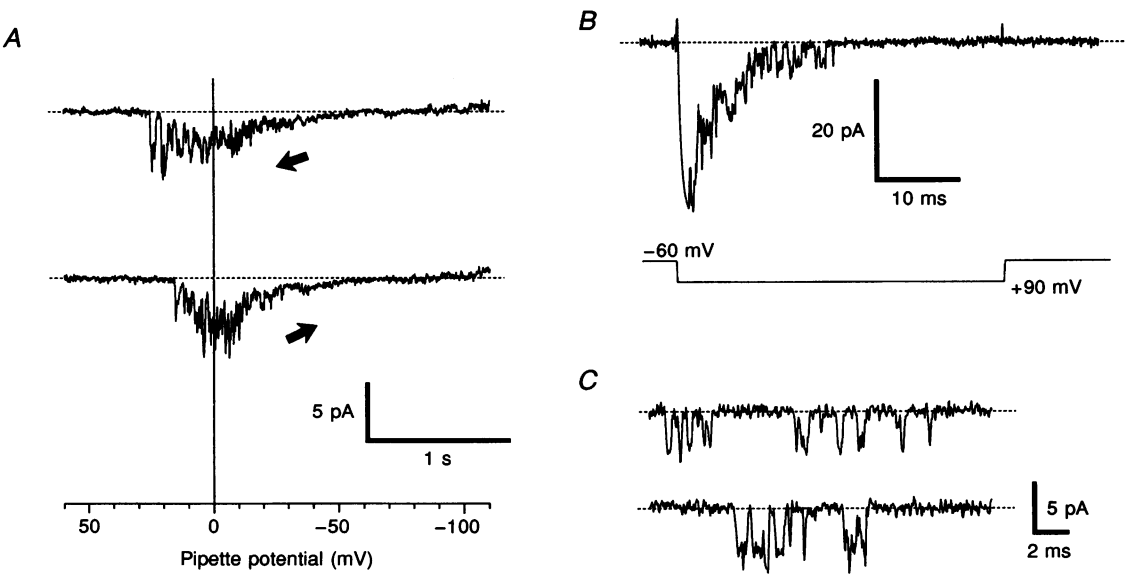

Figure 6. Inactivating I_{K1} channel activity recorded in the cell-attached mode

A, *I–V* relationship of the patch membrane recorded by applying slow ramp waves. The direction of the potential change is marked by arrows. Records were filtered at 100 Hz and sampled at 500 Hz. The leak (27 GΩ) current was subtracted. *B*, current evoked by a hyperpolarizing potential step. The leak and capacitive currents were subtracted. *C*, single channel activity recorded during hyperpolarizing potential steps (pipette potentials of +60 and +120 mV). KCl solution (125 mM) was used in the pipette in *A*, *B* and *C*. Records were obtained in long spike-type hair cells.

The same channel activity was observed in cell-attached mode when either KCl, potassium acetate or potassium citrate solution was used, but was not observed when NaCl or CsCl solution was used. This indicated that K^+ carried the current through this channel. It is unclear why the reversal potential was much less negative than the resting potentials measured in the whole-cell clamp mode (−90 to −100 mV). One possible explanation is that the membrane potential of these cells was at a low negative plateau level. In experiments in the cell-attached mode, the resting transduction current, which may have been more intact than that in whole-cell recording, or the inward current which flowed through the I_{K1} channels in the patch membrane (cf. Ohmori, 1984), may have switched the membrane potential to the plateau level.

The same channel activity characterized by time-dependent decay was observed in inside-out patches in symmetrical 125 mM KCl solution. In this condition, single-channel activity was easily observed probably because of a decrease in the number of active channels due to run down, although all the channels eventually disappeared in tens of minutes. The activity showed time-dependent decay at −150 and −200 mV (Fig. 7*A*), similar to the findings in the cell-attached mode (Fig. 6*B*). The decay accelerated with increasing hyperpolarization (3·7 and 1·1 ms at −150 and −200 mV, respectively; Fig. 7*A*). This decay was due to a decrease in the probability of the occurrence of the open state with time. Similar decay has been observed in I_{K1} channels in ventricular myocytes (Sakmann & Trube, 1984). The *I–V* relationship of the single-channel current (Fig. 7*B*) showed a slope conductance of 27·7 ± 1·2 pS ($n = 3$), which was almost identical to that measured in the cell-attached mode. The extrapolated reversal potential was 0·4 ± 0·9 mV ($n = 3$). When depolarizing voltages were applied from a holding potential of 0 mV, we could not see any clear open events (Fig. 7*C*) although nominally Mg^{2+}-free KCl solution was used on both sides of the patch membrane.

The channel with activity recorded in the cell-attached and inside-out modes is very likely to carry I_{K1} for several reasons. (1) This channel was a K^+ channel with inwardly rectifying characteristics. (2) This channel was present in abundance in long spike-type hair cells, but was not

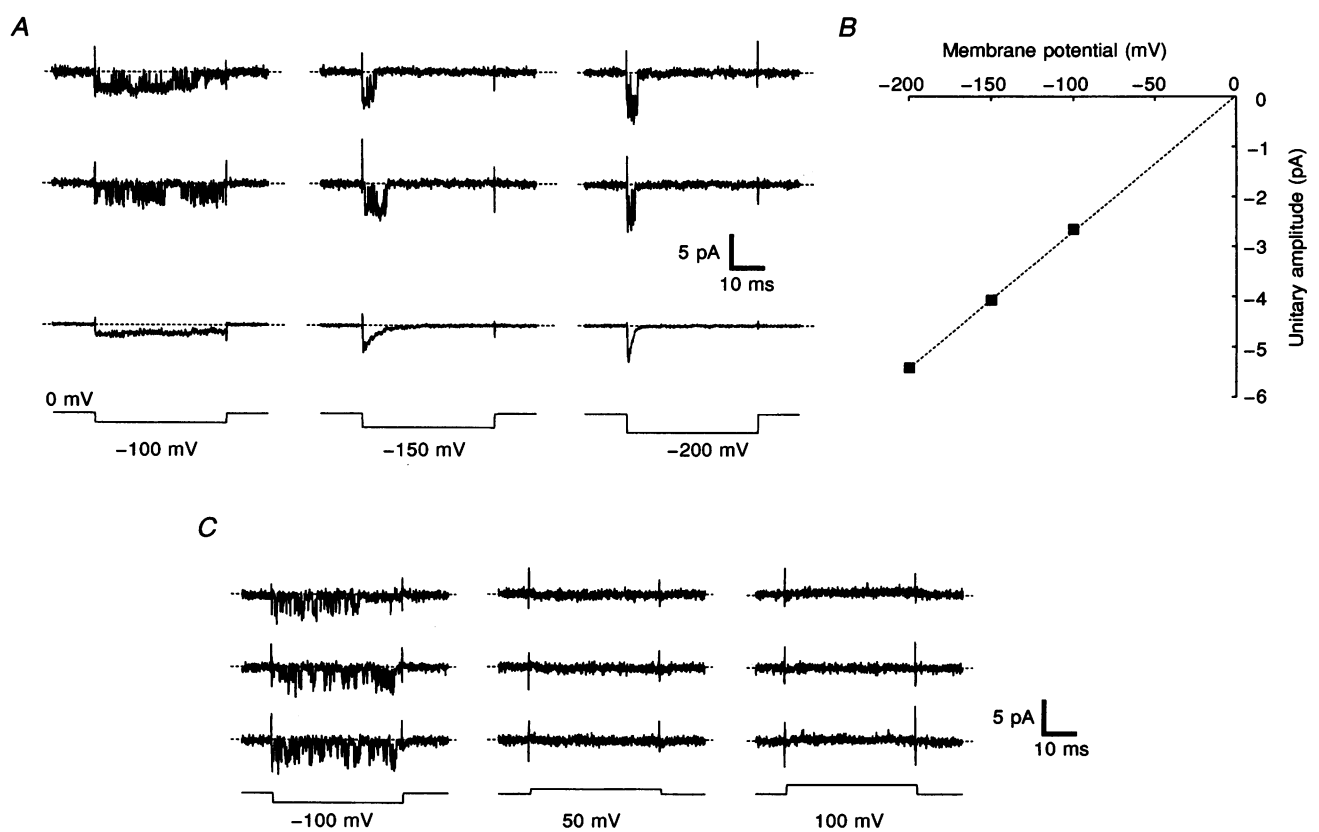

Figure 7. I_{K1} channel activity recorded in the inside-out mode

A, response to hyperpolarizing potential steps in sample records (top 2 traces) and the average of 20 traces (middle). The time-dependent decay phase in the average traces with −150 and −200 mV steps could be fitted by single-exponential curves with time constants of 3·7 and 1·1 ms, respectively. *B*, *I–V* relationship of single-channel amplitude. The straight line fitted by the least-squares method had a slope conductance of 26 pS and a reversal potential of −1 mV. *C*, response to hyperpolarizing and depolarizing potential steps recorded in another membrane patch. The pipette and bath contained 125 mM KCl solution.

observed in short oscillatory-type hair cells which lacked I_{K1} (see the later section on I_h single-channel current). (3) This channel showed time-dependent decay (inactivation) with increasing hyperpolarization. Therefore, we refer to this channel as a decaying-type (or inactivating-type) I_{K1} channel.

This channel activity decayed almost completely with strong hyperpolarization (Figs 6*A*, *B* and 7*A*), while I_{K1} in the whole-cell condition did not decay completely, even with strong hyperpolarization (e.g. −200 mV). This discrepancy could not be resolved in the present study. It may be possible that a different ionic composition (high K^+ and zero Na^+ external concentrations in the cell-attached and inside-out modes) could change the decay kinetics of decaying-type I_{K1} channels or alternatively, I_{K1} could be carried by decaying-type channels along with other non-decaying inwardly rectifying K^+ channels.

Non-decaying inwardly rectifying channels were occasionally recorded in long spike-type hair cells in the cell-attached mode. We previously reported 'quickly flickering' channels (Sugihara & Furukawa, 1986). However, further experiments indicated that 'quickly flickering' channels were found much less frequently than decaying-type I_{K1} channels. The latter had been difficult to recognize at first because a clear single-channel activity was not seen with the pipette potentials held constant (cf. Fig. 6*A*). Another inwardly rectifying channel with a slower gating speed and a conductance of 23·6 ± 1·5 pS ($n = 5$, with 125 mM KCl pipette solution) was also recorded. However, since the activity of these non-inactivating channels was much less frequently observed than that of decaying-type I_{K1} channels, these non-inactivating channels does not seem to explain the non-inactivating portion of I_{K1} recorded in the whole-cell mode.

When I_{K1} was recorded in the whole-cell voltage-clamp mode with Cs^+ internal solution, complete time-dependent decay during hyperpolarizing potential steps (< −130 mV) together with a general rightward shift of the *I–V* relationship was observed (not shown). This suggested that the kinetics of the time-dependent decay of I_{K1} may be affected by the internal and external concentrations of K^+ and other ions. Ohmori (1984) has suggested that internal Cs^+ interacts with the I_{K1} channel.

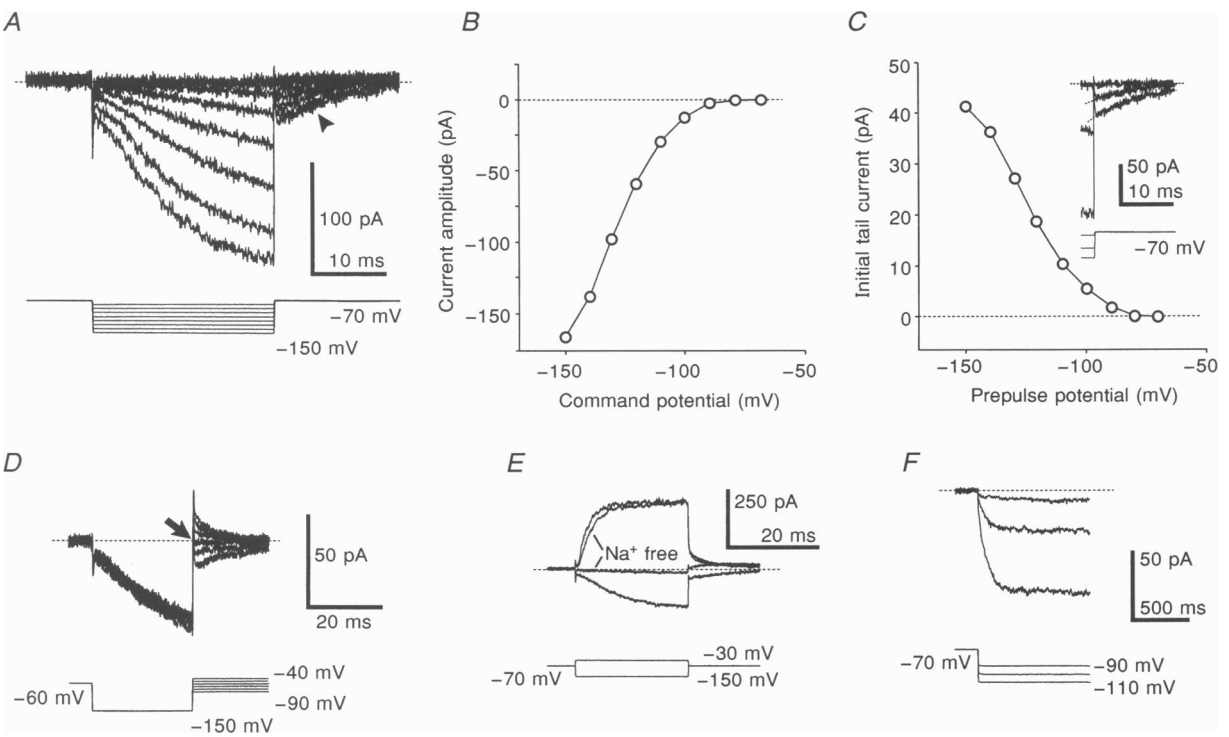

Figure 8. Hyperpolarization-activated potassium–sodium current (I_h) in oscillatory-type hair cells

A, I_h evoked by hyperpolarizing potential steps (amplitude, −10 to −80 mV) applied from a holding potential of −70 mV. The arrowhead indicates tail current. *B*, *I–V* curve measured at the end of the potential steps from the records in *A*. *C*, amplitude of the initial tail current plotted against the prepulse potential measured using the data depicted in *A*. *D*, reversal of the tail current of I_h. The trace with the flattest tail current is marked by an arrow. *E*, records before and after replacing Na^+ in the bath with choline. *F*, activation of I_h with a slow time scale. Potential steps 1 s in duration were applied. Records were filtered at 100 Hz and sampled at 500 Hz. All the records in this figure were obtained in short oscillatory-type hair cells in the caudal sacculus. KCl internal solution was used in *A–C*, and potassium citrate internal solution was used in *D*, *E* and *F*. See text for the composition of the bath solution used in *D*.

Characterization of hyperpolarization-activated potassium–sodium current (I_h)

Most short oscillatory-type hair cells have hyperpolarization-activated inwardly rectifying currents similar to I_h found in photoreceptors (Sugihara & Furukawa, 1989, 1995). The biophysical properties of this current were further investigated in the present study. A gradual slow time course of activation (Fig. 8*A*) was characteristic of this current and was distinguishable from the faster activation of inwardly rectifying K^+ current (I_{K1}) in spike-type hair cells (cf. Fig. 4*A*). The *I–V* relationship (Fig. 8*B*) and voltage-activation curve obtained by measuring the initial tail current (Fig. 8*C*) showed a voltage range of activation which was more negative than −80 mV. No saturation was seen in the voltage-activation curve even at −150 mV (Fig. 8*C*), although this curve did not necessarily represent the steady state because the prepulse was not long enough (25 ms). The tail current of I_h flowed inwardly at −70 mV under normal recording conditions (internal KCl and external normal Ringer solution; Fig. 8*A* arrowhead). The appearance of this current did not depend on whether Cl^- or citrate was used in the internal solution (KCl in Fig. 8*A*, potassium citrate in Fig. 8*D*, *E* and *F*), which suggests the passage of cations. The reversal potential of this current was measured using modified K^+-free Ringer solution (10 mM $MgCl_2$, 10 mM 4-AP, 30 mM TEA, 72·5 mM NaCl and 5 mM Hepes–NaOH, with the pH adjusted to 7·2) in the bath (Fig. 8*D*). This bath solution should shift the reversal potential in the negative direction and prevent Ca^{2+} current, if there is any, and outward K^+ currents from being activated even when repolarizing pulses less negative than the holding potential were applied. A reversal potential of −70 mV was obtained under these conditions. By assuming that Na^+ and K^+ carry this current, the relative permeability of Na^+ *versus* K^+ calculated according to the Goldman–Hodgkin–Katz equation was 0·14. This value was not dissimilar to those reported in salamander rod photoreceptors (0·2, 0·25 and 0·3 with 2, 5 and 10 mM K_o^+, respectively; Hestrin, 1987) if we consider the dependence of the relative permeability of Na^+ *versus* K^+ on $[K^+]_o$ (Hestrin, 1987). However, the relative permeability of I_h in the standard recording condition (2 mM K_o^+) should be greater than 0·14. Thus, the reversal potential may be less negative than −47 mV, which was calculated for a relative permeability of 0·14. The reversal potential of I_h in the present study is not very different from those of photoreceptors (−30 mV; Hestrin, 1987) and thalamic relay neurons (−43 mV; McCormick & Pape, 1990) that were measured using solutions of physiological composition. These similarities between the important biophysical properties of the present current and those of I_h in other preparations led us to apply the name 'I_h.'

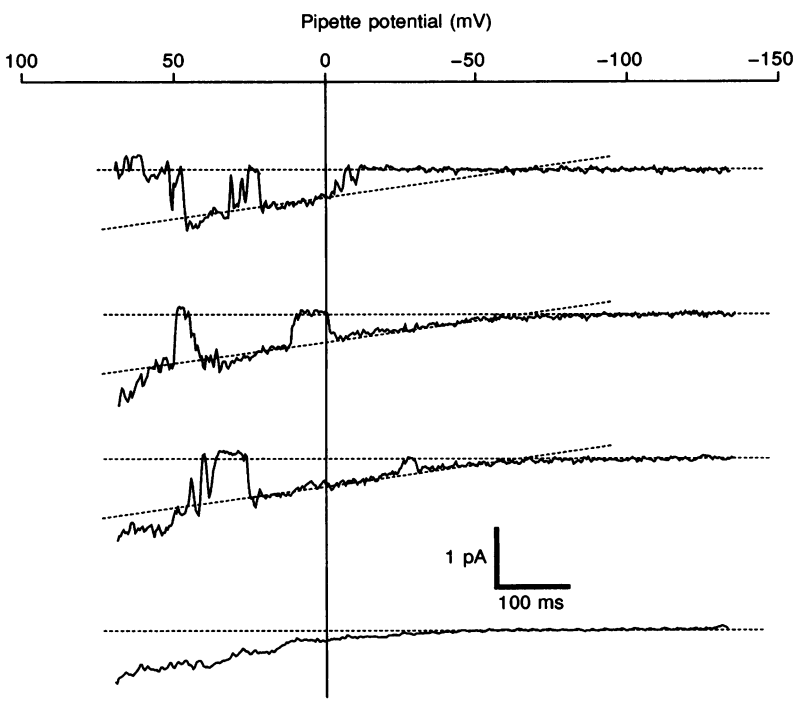

Figure 9. Activity of the single putative I_h channel recorded in the cell-attached mode

Current response to a slow ramp wave (+70 to −130 mV in pipette potential) was filtered at 100 Hz and sampled at 500 Hz. The leak current (51 GΩ) was subtracted so that the shut state would remain level (horizontal dashed lines). The slanting dashed lines, which reflect a single-channel conductance of 6·9 pS and a reversal potential of −68 mV (pipette potential), were identical and drawn by eye to fit the open level of all 3 traces. The bottom trace is the average of 16 individual traces obtained with either depolarizing or hyperpolarizing ramp waves. The pipette solution was potassium acetate. Traces were recorded in a short oscillatory-type hair cell.

Although K^+ is more permeable than Na^+, most of I_h was carried by Na^+, since the driving force for Na^+ is much stronger at the hyperpolarized range of the membrane potential (−90 to −150 mV). This was experimentally proven by the suppression of I_h by replacing Na^+ in the bath with choline (Fig. 8*E*). Outward K^+ current ($I_{A(H)}$, Sugihara & Furukawa, 1995) was not affected very much by this replacement (Fig. 8*E*). In addition, removal of external K^+ did not suppress I_h significantly (Sugihara & Furukawa, 1989).

When a long command pulse was applied, activation of I_h reached a plateau in about 200 ms with an activation time constant of 77 ms at −100 mV (Fig. 8*F*). This activation time constant was not very different from that of photoreceptors (about 50 ms at −100 mV; Hestrin, 1987) or thalamic neurons (229 ms at −95 mV; McCormick & Pape, 1990). The time constant of tail decay was 8–12 ms.

I_h channel activity recorded in the cell-attached mode

We attempted to record single-channel current of I_h in the cell-attached mode in short oscillatory-type hair cells. Decaying-type I_{K1} channels were not observed in these hair cells ($n = 26$). However, different channels were occasionally recorded when the patch membrane was hyperpolarized in the cell-attached mode ($n = 5$ out of 26). This activity was characterized by relatively slow open and shut events of small inward current when the patch membrane was hyperpolarized (Fig. 9). In one case in which the noise level was low and a single channel was present, the measured unitary conductance was 6·9 pS and the reversal potential was −68 mV (Fig. 9). Since the pipette solution was potassium acetate, the inward current was presumably carried by an influx of K^+. The reversal potential was close to the resting potential of short oscillatory-type hair cells (about −75 mV, Sugihara & Furukawa, 1989) and hence close to the equilibrium potential for K^+ under these conditions. The average *I–V* curve had a convex shape (Fig. 9, bottom trace), indicating hyperpolarization-dependent activation. Since these findings coincide with the characteristics of I_h, this may have been the activity of I_h channels.

DISCUSSION

Different inwardly rectifying currents in hair cells and supporting cells

The present study revealed the biophysical properties of different inwardly rectifying currents in hair cells and supporting cells in the goldfish sacculus. Except for a report on Hensen cells isolated from guinea-pig cochlea, which noted the presence of an inward rectifier current as well as a delayed outward rectifier current (Santos-Sacchi, 1991), this paper presents the first characterization of an ionic current in a supporting cell. While I_{K1} in spike-type cells and I_{sc} in supporting cells were primarily selective for K^+, I_h in oscillatory type hair cells was permeable to K^+ and Na^+.

Conventional inwardly rectifying K^+ currents (I_{K1}) recorded in skeletal muscle (Standen & Stanfield, 1979), cardiac cells (Carmeliet, 1982; Sakmann & Trube, 1984) and tunicate oocytes (Ohmori, 1978) are characterized by relatively strict inward rectification and time-dependent decay at very negative voltages (< −150 mV). Identical or very similar currents have been found in many other cells, including oligodendrocytes (Barres, Chun & Corey, 1988), astrocytes (Ransom & Sontheimer, 1995), Müller cells (Newman, 1993), chick vestibular hair cells (Ohmori, 1984), tall hair cells in the apical part of the chick cochlea (Fuchs & Evans, 1990) and cylindrically shaped hair cells in the frog sacculus (Holt & Eatock, 1995). I_{K1} in spike-type hair cells in the goldfish sacculus also had characteristics similar to these currents in various tissues. On the other hand, I_{sc} in supporting cells was a unique K^+ current which showed biophysical properties that were clearly different from those of conventional I_{K1}. Time-dependent decay was not seen in I_{sc} at high negative voltages. Inward rectification of I_{sc} was not as strict as that of I_{K1}. In this regard, I_{sc} is similar to other weakly inwardly rectifying K^+ currents, such as those carried by the ROMK1 channel (Nichols, Ho & Hebert, 1994) and ATP-sensitive K^+ channels (Kakei & Noma, 1984).

Physiological role played by supporting cells

In the goldfish saccular macula, the entire basolateral membrane of hair cells is surrounded by supporting cells which are taller than hair cells to make contact with the basal lamina (Hama, 1969). Presumably, supporting cells occupy a larger volume than hair cells in the sensory epithelium. Therefore, supporting cells seem suitable for a K^+-buffering function. The slowly depolarizing DC response during sound stimulation in supporting cells in the goldfish sacculus (Furukawa, 1985) and guinea-pig cochlea (Oesterle & Dallos, 1990) has suggested the presence of K^+-conductance and K^+-buffering functions in these supporting cells.

First, selective permeation of K^+ is important for excessive K^+ in the extracellular space to enter supporting cells. The resting membrane potential, which should be close to the I_{sc} reversal potential, may be more positive than the K^+ equilibrium potential (E_K) by about 10–20 mV because the K^+ *versus* Na^+ permeability ratio of I_{sc} was about 30 : 1, which is smaller than that of Müller cell I_{K1} (435 : 1, Newman, 1985). Therefore, it would be necessary for local $[K^+]_o$ to increase by 1·5–2·5-fold (shift in local E_K by 10–20 mV) to allow K^+ to enter supporting cells through I_{sc} if the resting membrane potential is constant. An increase in the local $[K^+]_o$ of 5·3 mM during strong sound stimulation was estimated by Furukawa (1985) in the rostral sacculus. The local $[K^+]_o$ in the caudal sacculus, where the supporting cells in the present study were obtained, has not yet been determined experimentally. However, if an increase in local $[K^+]_o$ comparable to that in the rostral sacculus can be assumed, K^+ may enter supporting cells through the I_{sc} current in the caudal sacculus.

Another requirement for K^+ to enter supporting cells is that the change in the membrane potential should be much smaller than the increase in the local E_K so that the local E_K can exceed the membrane potential. If we assume an even distribution of ion channels, the membrane potential of a given supporting cell would be determined mainly in the surface area facing the basilar lamina and other supporting cells because this area is much greater than the rest of the surface area facing hair cells. In this situation, an increase in $[K^+]_o$ in the extracellular space between a supporting cell and a hair cell would not significantly affect the supporting cell membrane potential, but would only increase the local E_K. Locally excessive extracellular K^+ could then enter supporting cells. In addition, the gap junction between supporting cells (Hama & Saito, 1977) tends to keep the membrane potential of connected cells similar (Santos-Sacchi & Dallos, 1983; Santos-Sacchi, 1991). This effect would also reduce the change in the supporting cell membrane potential and favours K^+ influx into supporting cells due to an increase in the local $[K^+]_o$.

A characteristic of I_{sc} is weak inward rectification. The efflux of K^+ through outward I_{sc} might be functionally important. Fish endolymph contains a high concentration of Na^+ (Enger, 1964; Matsuura, Ikeda & Furukawa, 1971). Since Na^+ enters through the transduction channel together with K^+ (Corey & Hudspeth, 1979) while only K^+ leaves the cell through outward K^+ current, significant Na^+ accumulation occurs after large and/or persistent sound stimulation. Na^+ influx also occurs through non-electrogenic transport systems in the basolateral membrane (Mroz, Nissim & Lechene, 1993). Hair cells would have to uptake K^+ from the basolateral extracellular space and expel Na^+ through the Na^+–K^+ pump. The fact that hair cells have a large number of mitochondria (Hama, 1969), and that application of ouabain to the perilymph reduces microphonic potentials in goldfish sacculus (Matsuura *et al.* 1971), agrees with this idea of the uptake of K^+ by hair cells. A significant activity of the Na^+–K^+ pump has recently been confirmed in goldfish hair cells (Mroz *et al.* 1993). In this case, the weak inward rectification of supporting cell I_{sc} would be very convenient because it could supply K^+ to the extracellular space through outward current flow through I_{sc}. In conclusion, I_{sc} is likely to give supporting cells a certain K^+-buffering function in both influx and efflux.

Role of I_{K1} in spike-type hair cells

The physiological function of I_{K1} would be to stabilize the very negative resting potential, as indicated previously (Sugihara & Furukawa, 1989; Fuchs & Evans, 1990; Holt & Eatock, 1995), since this current is active at that voltage range (Fig. 4*C*). In addition, the strict inward rectification of I_{K1} enable the generation of low negative plateau potentials in spike-type hair cells, as demonstrated in this study (Fig. 5).

The most likely candidate for the inward current that can trigger the generation of spikes from the very negative resting potential and keep the membrane at the plateau level under physiological conditions, is the transduction current, because a small transduction current flows at the resting position of the hair bundle (Hudspeth & Corey, 1977). In the isolated preparation under whole-cell recordings, the transduction current may be partially damaged, since the transduction conductance we recorded was at best about 500 pS, and much smaller in most cases (I. Sugihara & T. Furukawa, unpublished observations). When the membrane potential is in the very negative resting level, a sufficiently large inward transduction current would immediately trigger spike generation, since the Na^+ current underlying spike generation (Sugihara & Furukawa, 1989) is largely released from inactivation at the high negative resting potential. After the spike, the membrane potential would remain at the low negative plateau level if the inward transduction current persists. Ca^{2+} current did not seem to contribute to maintaining the plateau potential (Fig. 5*D*) because it is scarcely activated at −60 or −50 mV in hair cells (Ohmori, 1984; Sugihara & Furukawa, 1989). On the other hand, K^+ conductances would induce the membrane potential to return to the very negative resting level. One such conductance is the K^+ conductance activated by efferent inhibitory synaptic input, as demonstrated in chick hair cells (Shigemoto & Ohmori, 1991; Fuchs & Murrow, 1992). Another K^+ conductance is the tail current of the outward K^+ current which would be activated if large depolarization occurs. It seems that if this tail current is sufficiently large, repetitive spikes (Sugihara & Furukawa, 1989) would be generated when current injection is continued.

The above points suggest that the membrane potential of spike-type hair cells in the saccular macula may frequently be at the plateau level. A response (receptor potential) to the sound stimulus would be depolarization from the low negative level, which would be convenient for releasing the transmitter. This mechanism may be significant because afferent fibres ('S2') which innervate the caudal sacculus, in which spike-type hair cells are abundant, have even higher sensitivity than other fibres ('S1') which innervate the rostral sacculus (Furukawa & Ishii, 1967).

Single-channel current of I_{K1}

Single-channel currents corresponding to I_{K1} were recorded under both cell-attached and inside-out conditions in the present study. Similar channels have been recorded in chick hair cells in the cell-attached mode (Ohmori, 1984). It is generally thought that the time-dependent decay of inwardly rectifying K^+ current is due to blocking by external Na^+ (Ohmori, 1978; Standen & Stanfield, 1979; Ohmori, 1984). However, we observed the time-dependent decay of I_{K1} single-channel current in both the inside-out and cell-attached modes, in which K^+ is the sole external cation. The decay may be explained as inactivation, i.e. an

intrinsic gating property of the I_{K1} channel, as suggested in ventricular myocytes (Sakmann & Trube, 1984; Koumi, Sato & Hayakawa, 1994), and/or blockade by K^+ itself, as suggested in pigmented ciliary epithelial cells (Stelling & Jacob, 1992). With regard to outward current, cardiac I_{K1} and cloned IRK1 channels pass outward current if the internal side is free of Mg^{2+} (Matsuda *et al.* 1987; Taglialatela, Wible, Caporaso & Brown, 1994). We did not observe similar events (Fig. 7*C*). Inactivation of the channel at a holding potential of 0 mV might explain the present results.

Similar correlation of I_h and I_{K1} expression with the shape of hair cells in the goldfish and frog sacculus

In our previous study on isolated goldfish saccular hair cells, we presented the first evidence for the existence of I_h-like current in short hair cells (Sugihara & Furukawa, 1989). The present study identified this current as I_h, which has been reported in photoreceptors and other cells based on their similar biophysical properties. Holt & Eatock (1995) recently identified I_h in leopard frog saccular hair cells. In goldfish saccular hair cells, I_h was seen in 86% of short oscillatory-type hair cells (Sugihara & Furukawa, 1995) and was not observed in long spike-type hair cells (e.g. Fig. 4*D*). In contrast, I_h was seen in all the hair cells in the leopard frog sacculus. However, the other inwardly rectifying current, I_{K1}, was seen only in cylindrical hair cells with a smaller width : length ratio in the leopard frog sacculus (Holt & Eatock, 1995). This seems to be remarkably similar to the situation in goldfish saccular hair cells, in which I_{K1} is expressed only in long spike-type hair cells (Sugihara & Furukawa, 1989). Thus, the correlation between the shape of the hair cells and ionic currents that was first reported in goldfish saccular hair cells (Sugihara & Furukawa, 1989) may also be present in other species. The different types of hair cells in the goldfish sacculus are distributed differently in the rostral and caudal macula and are presumably related to different response properties of auditory afferents innervating the rostral and caudal sacculus (Furukawa & Ishii, 1967; Sugihara & Furukawa, 1989, 1995).

Barres, B. A., Chun, L. L. Y. & Corey, D. P. (1988). Ion channel expression by white matter glia: I. type 2 astrocytes and oligodendrocytes. *Glia* **1**, 10–30.

Carmeliet, E. (1982). Induction and removal of inward-going rectification in sheep cardiac Purkinje fibres. *Journal of Physiology* **327**, 285–308.

Corey, D. P. & Hudspeth, A. J. (1979). Ionic basis of the receptor potential in a vertebrate hair cell. *Nature* **281**, 675–677.

Dempster, J. (1993). *Computer Analysis of Electrophysiological Signals.* Academic Press, London.

Enger, P. S. (1964). Ionic composition of the cranial and labyrinthine fluids and saccular D.C. potentials in fish. *Comparative Biochemistry and Physiology* **11**, 131–137.

Fuchs, P. A. & Evans, M. G. (1990). Potassium currents in hair cells isolated from the cochlea of the chick. *Journal of Physiology* **429**, 529–551.

Fuchs, P. A. & Murrow, B. W. (1992). Cholinergic inhibition of short (outer) hair cells of the chick's cochlea. *Journal of Neuroscience* **12**, 800–809.

Furukawa, T. (1985). Slow depolarizing response from supporting cells in the goldfish saccule. *Journal of Physiology* **366**, 107–117.

Furukawa, T. & Ishii, Y. (1967). Neurophysiological studies on hearing in goldfish. *Journal of Neurophysiology* **30**, 1377–1403.

Hama, K. (1969). A study on the fine structure of the saccular macula of the gold fish. *Zeitschrift für Zellforschung und Microskopische Anatomie* **94**, 155–171.

Hama, K. & Saito, K. (1977). Gap junctions between the supporting cells in some acoustico-vestibular receptors. *Journal of Neurocytology* **6**, 1–12.

Hestrin, S. (1987). The properties and function of inward rectification in rod photoreceptors of the tiger salamander. *Journal of Physiology* **390**, 319–333.

Holt, J. R. & Eatock, R. A. (1995). Inwardly rectifying currents of saccular hair cells from the leopard frog. *Journal of Neurophysiology* **73**, 1484–1502.

Hudspeth, A. J. & Corey, D. P. (1977). Sensitivity, polarity, and conductance change in the response of vertebrate hair cells to controlled mechanical stimuli. *Proceedings of the National Academy of Sciences of the USA* **74**, 2407–2411.

Kakei, M. & Noma, A. (1984). Adenosine-5′-triphosphate-sensitive single potassium channel in the atrioventricular node cell of the rabbit heart. *Journal of Physiology* **352**, 265–284.

Koumi, S., Sato, R. & Hayakawa, H. (1994). Modulation of voltage-dependent inactivation of the inwardly rectifying K^+ channel by chloramine-T. *European Journal of Pharmacology* **258**, 281–284.

Lopatin, A. N., Makhina, E. N. & Nichols, C. G. (1994). Potassium channel block by cytoplasmic polyamines as the mechanism of intrinsic rectification. *Nature* **372**, 366–369.

Matsuda, H., Saigusa, A. & Irisawa, H. (1987). Ohmic conductance through the inwardly rectifying K channel and blocking by internal Mg^{2+}. *Nature* **325**, 156–159.

Matsuura, S., Ikeda, K. & Furukawa, T. (1971). Effects of Na^+, K^+, and ouabain on microphonic potentials of the goldfish inner ear. *Japanese Journal of Physiology* **21**, 563–578.

McCormick, D. A. & Pape, H.-C. (1990). Properties of a hyperpolarization-activated cation current and its role in rhythmic oscillation in thalamic relay neurons. *Journal of Physiology* **431**, 291–318.

Mroz, E. A., Nissim, K. R. & Lechene, C. (1993). Rapid resting ion fluxes in goldfish hair cells are balanced by (Na^+, K^+)-ATPase. *Hearing Research* **70**, 22–30.

Newman, E. A. (1985). Membrane physiology of retinal glial (Müller) cells. *Journal of Neuroscience* **5**, 2225–2239.

Newman, E. A. (1993). Inward-rectifying potassium channels in retinal glial (Müller) cells. *Journal of Neuroscience* **13**, 3333–3345.

Nichols, C. G., Ho, K. & Hebert, S. (1994). Mg^{2+}-dependent inward rectification of ROMK1 potassium channels expressed in *Xenopus* oocytes. *Journal of Physiology* **476**, 399–409.

Oesterle, E. C. & Dallos, P. (1990). Intracellular recordings from supporting cells in the guinea pig cochlea: DC potentials. *Journal of Neurophysiology* **64**, 617–636.

Ohmori, H. (1978). Inactivation kinetics and steady-state current noise in the anomalous rectifier of tunicate egg cell membranes. *Journal of Physiology* **281**, 77–99.

OHMORI, H. (1984). Studies of ionic currents in the isolated vestibular hair cell of the chick. *Journal of Physiology* **350**, 561–581.

ORKAND, R. K., NICHOLLS, J. G. & KUFFLER, S. W. (1966). Effect of nerve impulses on the membrane potential of glial cells in the central nervous system of amphibia. *Journal of Neurophysiology* **29**, 788–806.

RANSOM, C. B. & SONTHEIMER, H. (1995). Biophysical and pharmacological characterization of inwardly rectifying K^+ currents in rat spinal cord astrocytes. *Journal of Neurophysiology* **73**, 333–346.

SAKMANN, B. & TRUBE, G. (1984). Voltage-dependent inactivation of inward-rectifying single-channel currents in the guinea-pig heart cell membrane. *Journal of Physiology* **347**, 659–683.

SANTOS-SACCHI, J. (1991). Isolated supporting cells from the organ of Corti: Some whole cell electrical characteristics and estimates of gap junctional conductance. *Hearing Research* **52**, 89–98.

SANTOS-SACCHI, J. & DALLOS, P. (1983). Intercellular communication in the supporting cells of the organ of Corti. *Hearing Research* **9**, 317–326.

SHIGEMOTO, T. & OHMORI, H. (1991). Muscarinic receptor hyperpolarizes cochlear hair cells of chick by activating Ca^{2+}-activated K^+ channels. *Journal of Physiology* **442**, 669–690.

STANDEN, N. B. & STANFIELD, P. R. (1979). Potassium depletion and sodium block of potassium currents under hyperpolarization in frog sartorius muscle. *Journal of Physiology* **294**, 497–520.

STELLING, J. W. & JACOB, T. J. C. (1992). The inward rectifier K^+ current underlies oscillatory membrane potential behaviour in bovine pigmented ciliary epithelial cells. *Journal of Physiology* **458**, 439–456.

SUGIHARA, I. (1994) Calcium-activated potassium channels in goldfish hair cells. *Journal of Physiology* **476**, 373–390.

SUGIHARA, I. & FURUKAWA, T. (1986). Quickly flickering inwardly rectifying K channels in goldfish hair cell membrane. *Neuroscience Research* **3**, 261–267.

SUGIHARA, I. & FURUKAWA, T. (1989). Morphological and functional aspects of two different types of hair cells in the goldfish sacculus. *Journal of Neurophysiology* **62**, 1330–1343.

SUGIHARA, I. & FURUKAWA, T. (1995). Potassium currents underlying the oscillatory response in hair cells of the goldfish sacculus. *Journal of Physiology* **489**, 443–453.

TAGLIALATELA, M., WIBLE, B. A., CAPORASO, R. & BROWN, A. M. (1994). Specification of pore properties by the carboxyl terminus of inwardly rectifying K^+ channels. *Science* **264**, 844–847.

Acknowledgements

This study was supported by Grants-in-Aid for Scientific Research from the Ministry of Education, Science and Culture of Japan.

Author's email address

I. Sugihara: isugihara.phy1@med.tmd.ac.jp

Received 11 December 1995; accepted 6 June 1996.